
Title: *NNN*-Pincer-Copper Complex Immobilized on Magnetic Nanoparticles as a Powerful Hybrid Catalyst for Aerobic Oxidative Coupling and Cycloaddition Reactions in Water

Author: Nasrin Zohreh Mahboobeh Jahani

PII: S1381-1169(16)30481-2
DOI: http://dx.doi.org/doi:10.1016/j.molcata.2016.11.007
Reference: MOLCAA 10104

To appear in: *Journal of Molecular Catalysis A: Chemical*

Received date: 12-9-2016
Revised date: 28-10-2016
Accepted date: 5-11-2016

Please cite this article as: Nasrin Zohreh, Mahboobeh Jahani, NNN-Pincer-Copper Complex Immobilized on Magnetic Nanoparticles as a Powerful Hybrid Catalyst for Aerobic Oxidative Coupling and Cycloaddition Reactions in Water, Journal of Molecular Catalysis A: Chemical http://dx.doi.org/10.1016/j.molcata.2016.11.007

# *NNN*-Pincer-Copper Complex Immobilized on Magnetic Nanoparticles as a Powerful Hybrid Catalyst for Aerobic Oxidative Coupling and Cycloaddition Reactions in Water

Nasrin Zohreh,* Mahboobeh Jahani

[a] *Department of Chemistry, Faculty of Science, University of Qom, P. O. Box: 37185-359, Qom, Iran*

Graphical abstract

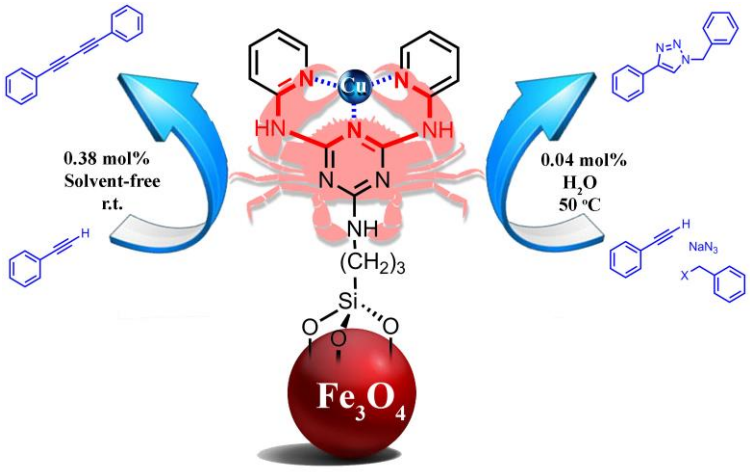


Highlights:

- Easy preparation of magnetic *NNN*-pincer copper catalyst as heterogeneous catalyst
- High loading 0.38 mmol.g$^{-1}$ of Cu(I) on heterogeneous support because of powerful pincer ligand
- Successful application of the catalyst to variety of substrates for homocoupling and click reactions in water using 0.38 and 0.04 mol% catalyst loading
- Recoverable and reusable up to 8 times without leaching and reduced activity

**Abstract**

A simple and reliable methodology is described for preparing the first heterogeneous *NNN*-pincer-copper hybrid catalyst with a high control over surface composition. The strategy relies on the covalently bonding of 2-aminopyridine to cyanuric chloride-functionalized magnetic nanoparticles followed by complexation with CuI. These claims are confirmed by different characterization methods such as SEM, TEM, FT-IR, TGA, ICP, XRD, and elemental analysis. The finely engineered supported catalyst is employed in the aerobic oxidative coupling of terminal alkynes and click reaction using only 0.38 and 0.04 mol% catalyst, respectively. All reactions perform under solvent-free condition or green solvent $H_2O$. Also, the catalyst is readily recovered and reused for up to 8 and 6 subsequent runs in click and homocoupling reactions without significant loss of activity or leaching.

**Keywords**

*NNN*-Pincer catalyst, copper catalyst, heterogeneous catalyst, cyanuric chloride, terminal alkyne homocoupling, click reaction

## Introduction

Pincer ligands are extensively used in many diverse areas of chemistry primarily as a means to direct and modulate the properties of a metal center to which it is bonded (Scheme 1).[1-4] Prof. Shaw, together with Dr. C.J. Moulton,[5] were the first ones to report examples of pincer compounds. However, the term "pincer" was first coined by van Koten in 1989 because of its similarity to a wretch or spanner.[6]

An important characteristic of the pincer platforms is the fact that its three ligating sites are well organized by the backbone of the ligand which leads to the possible formation of five- or six-membered chelate rings in which the central metal-heteroatom bond is in common (Scheme 1). Up to now, a multifaceted combination of donor sets has been explored that includes combinations of, e.g., neutral, anionic, Lewis basic and acidic, arene, heteroaromatic, and carbine donors.[7-11] Moreover, in some cases, the pincer platform itself acts as a non-innocent ligand (NIL) or provides, with its pincer-metal manifold, a system that is suitable for executing metal-ligand cooperative (MLC) behavior in, e.g., catalytic processes.[12, 13] At present, considering the wide range of metals, the number of possibilities seems to have no limit; most excitingly, many of these novel pincer ligand/metal combinations lead to the discovery of new catalysts for various bond formation processes in organic synthesis,[14-16] new polymerization technologies,[17] the chemical conversion of $CO_2$,[18] and the activation of bonds that so far were considered as primarily unreactive.[19, 20]

Among numerous metal-EZE' pincer catalysts, catalysts with pincer ligands of the type *NNN* (symmetric or unsymmetric, neutral or anionic) have been more considered because of the powerful chelating property of most metals.[21-25] In addition, designing a wide range of chiral

moiety bonded to each nitrogen atom makes metal-*NNN*-pincer complexes very applicable in asymmetric synthesis.[25-27]

After the introduction of heterogenization concept in the realm of catalysis science, thousand types of homogeneous catalysts have been immobilized on solid supports and applied in chemical reactions or industrial processes.[28] Recently, having considered the advantages of heterogeneous catalyst on the one hand, and unique and effective properties of pincer catalyst on the other hand, heterogenization of pincer catalysts has attracted much attention that could be interesting for modifying many chemical processes. The use of MOF,[29, 30] mesoporous silica,[31, 32] resins,[33] MNP,[34, 35] CNT,[36] and $SiO_2$[37] as solid supports for immobilization of pincer catalysts, are some examples. According to literature, there are a few reports on heterogeneous *NNN*-pincer catalyst.[34, 38]

Given these considerations and continuing our previous works,[39-41] we have investigated the immobilization of 2,4,6-trichloro-1,3,5-triazine (cyanuric chloride, TCT)-derived copper pincer complex onto the large surface area of highly dispersed magnetic nanoparticles. The catalytic activity of the resulting magnetic *NNN*-pincer copper catalyst is studied in both of terminal alkyne homocoupling and click reactions. To the best of our knowledge, there is no report on heterogeneous *NNN*-pincer copper catalyst.

## Experimental

### *Materials and methods*

Ferric chloride hexahydrate ($FeCl_3.6H_2O$), ferrous chloride tetrahydrate ($FeCl_2.4H_2O$), ammonia (25%), tetraethyl orthosilicate (TEOS), (3-aminopropyl)trimethoxysilane (APTS), and 2,4,6-trichloro-1,3,5-triazine (TCT) were obtained from Sigma-Aldrich without further purification.

*N*,*N*-Diisopropylethylamine (DIEA) was purchased from Merck and distilled before use. $Na_2WO_4$. $4H_2O$ and 2-aminopyridine were purchased from Merck. Various commonly used organic solvents (Merck) were dried with several different drying agents.

FT-IR spectra of samples were taken using an ABB Bomen MB-100 FT-IR spectrometer. Thermogravimetric analysis (TGA) was acquired under a nitrogen atmosphere with a TGA Q 50 thermogravimetric analyzer. Transmission electron microscopy (TEM) images were taken with a Philips CM30 electron microscope. Magnetization of catalyst was measured by vibrating sample magnetometer (Meghnatis Daghigh Kavir Co., Kashan, Iran). The X-ray diffraction (XRD) pattern was recorded on Rigaku D/Max-3c X-ray diffractometer. X-Ray fluorescence (XRF) was taken using Phillips 1404 XRF instrument. Atomic absorption spectrometry (AAS, Shimadzu 680 A) or inductively coupled plasma-optical emission spectrometry (ICP-AES, Perkin-Elmer DV 4300) were used for elemental measurements. CHN Elemental analyses were performed using a Heraeus Elemental Analyzer CHN (Elementar-Analysesysteme). Conversions and yields were measured using a 6890 gas chromatograph (GC) with an Agilent Technologies HP-Innowax.

*Preparation of amine functionalized magnetic nanoparticles (MNP@APTS)*

Silica coated $Fe_3O_4$ nanoparticles (MNPs) were synthesized based on our previously reported method.[42] Prepared MNPs (1.0 g) were ultrasonically dispersed in 50 mL ethanol/water (4/1) mixture. Then, APTS (5 mL) was added and the mixture was stirred at 80 °C for 24 h. The APTS coated magnetic nanoparticles (MNP@APTS, 1.0 g) were magnetically separated and washed several times with methanol (4 × 30 mL) and dried under vacuum at 50 °C.

*Synthesis of APTS-functionalized TCT (compound **1**)*

To a 50 mL flask containing TCT (1 mmol), DIPEA (1 mmol), and super dry THF (3 mL) in ice bath (-5 °C), APTS (1 mmol) was added dropwise. The reactants were vigorously stirred for 2 h. Then, the solvent was evaporated under vacuum at 50 °C. The crude product **1** was analyzed using $^{1}$H NMR spectrum.

*Preparation of pincer ligand TCT/Amp-functionalized magnetic nanoparticles (MNP@TCT/Amp)*

In a round bottom flask, MNP@APTS (1.0 g) was ultrasonically dispersed in dry THF (15 mL) and the flask was put in an ice bath. Then, TCT (5 mmol, 1.0 g) and DIEA (7 mmol, 1.2 mL) were added. The mixture was stirred for 2 h under $N_2$ atmosphere. The product (MNP@TCT) was magnetically separated and washed with THF (5×10 mL) and dried under vacuum at room temperature. In a three necked round bottom flask, MNP@TCT (0.98 g) was dispersed in dry $CH_3CN$ (25 mL) and 2-aminopyridine (4.5 mmol, 0.42 gr) was added to flask. The flask was equipped with a condenser and the mixture was refluxed for 12 h to produce MNP@TCT/Amp ligand. The heterogeneous ligand was separated using a magnet and washed with methanol (5×10 mL) and dried under vacuum at 50 ˚C (0.95 g).

*Preparation of NNN-pincer type nanomagnetic copper catalyst (MNP@NNN-Pincer/Cu)*

For complexation of MNP@TCT/Amp ligand with CuI, MNP@TCT/Amp (0.95 g) was dispersed in $CH_3CN$ (10 mL) and CuI (2 mmol, 0.38 g) was added to the mixture. The mixture was stirred for 12 h at room temperature. The final catalyst (MNP@ *NNN*-Pincer/Cu) was

magnetically separated and washed with $CH_3CN$ (2×10 mL), water (3×10 mL) and methanol (2×10 mL) and dried under vacuum at 50 ˚C (0.95 g).

*Synthesis of 2,4,6-tri(aminopyridinyl)-1,3,5-triazine ligand (ligand **A**)*

To a 50 mL flask containing TCT (5 mmol), DIPEA (25 mmol), and MeOH (8 mL) in ice bath (-5 °C), 2-aminopyridine (15 mmol) was added dropwise. The reactants were vigorously stirred for 2 h. Then, the temperature of the reaction was raised to 70 °C and the reaction refluxed for additional 12 h. Then, solvent was evaporated and the product **A** was washed with EtOH, $CHCl_3$, and $Et_2O$ and dried under vacuum.

*General procedure for aerobic oxidative homocoupling reaction of terminal alkyne*

Terminal alkyne (1 mmol), morpholine (1.2 mmol), and catalyst MNP@*NNN*-Pincer/Cu were loaded in a 25 mL round bottom flask. The reactants were vigorously stirred at room temperature (or 60 °C) for a defined time (the amount of catalyst loading and temperature were selected according to Table 3). Completion of the reaction was monitored by TLC until the initial alkyne consumed and no further product (comparing with the related known product by TLC) was formed. After completion of the reaction, methanol was added and the catalyst was magnetically separated, washed with methanol (3×10 mL) and dried for another run. The product mixtures were analyzed by gas chromatography (GC). The isolated yields of products were determined after purification of product using column chromatography (hexane/ethyl acetate as eluent).

*General procedure for azide/alkyne cycloaddition reaction (click reaction)*

Terminal alkyne (1 mmol), halide (1 mmol), $NaN_3$, $H_2O$ (2 mL), and catalyst MNP@ *NNN*-Pincer/Cu were loaded in a 25 mL round bottom flask. The reactants were vigorously stirred at 50 or 80 °C for the defined time (the amount of azide and catalyst loading were selected according to Tables 5, 6). Completion of the reaction was monitored by TLC until the initial alkyl halide and alkyne were consumed and no further product was formed (comparing with the related known product). Consuming of alkyl halide is not the only evidence for the completion of the reaction because the consumption of alkyl halide may be due to the formation of alkyl azide. Having completed the reaction, methanol (2 mL) was added and the catalyst was magnetically separated, washed with methanol (3×10 mL) and dried for another run. The product mixtures analyzed by gas chromatography (GC). In order to obtain isolated yield of products after completion of the reaction, the catalyst was magnetically separated and the reaction mixture was extracted with ethyl acetate. Solvent was evaporated and the product was recrystallized from ethyl acetate or purified using column chromatography (hexane/ethyl acetate as eluent).

*Reusability test of catalyst MNP@NNN-pincer/Cu in click reaction*

Phenylacetylene (5 mmol), alkyl halide (5 mmol), $NaN_3$ (6.5 mmol), $H_2O$ (2 mL), and catalyst MNP@ *NNN*-Pincer/Cu (0.04 mol%, 5 mg) were loaded in a test tube. The reactants were vigorously stirred at 50 °C for a defined time. After completion of the reaction, catalyst was carefully collected at the bottom of test tube using an external magnet and reaction mixture decanted in another pot. The catalyst was washed with MeOH (10 mL) and utilized directly in the next run without separation from test tube.

## Result and discussion

*Synthesis and characterization of catalyst*

Continuing our previous works on magnetic catalysts, here, we report a robust, simple and general methodology to easily get access to magnetic *NNN*-pincer copper catalyst. Initially, we supposed that 1,3,5-triazinetrichloride (cyanuric chloride, TCT) could serve as a core with three reactive sites that can bind to heterogeneous supports through substitution of one chloride and functionalize further through substitution of the other clorides.[43-45] We further took advantage of 2-aminopyridine as a powerful ligand[46, 47] while bonding to TCT. Accordingly, we designed the magnetic *NNN*-pincer copper catalyst MNP@*NNN*-pincer/Cu easily via a few steps as visualized in Scheme 2. First, magnetic $Fe_3O_4$ nanoparticles were synthesized by a co-precipitation method[48, 49] in the basic condition and covered by a silica layer to protect $Fe_3O_4$ from oxidative and acidic mediums. Then the surface of MNP was modified with APTS to provide amine group for further functionalization. Afterward, MNP@APTS was conducted to react with TCT via substitution of one Cl with amine group in the basic condition. Due to the high reactivity of TCT, this step was performed in ice bath using dry solvent to avoid further substitution of TCT. To ensure successful substitution of one Cl, the reaction of TCT with APTS was also carried out under similar condition according to Scheme 3 and the structure of product **1** was confirmed by NMR spectrum (Scheme 3). On the other hand, compound **1** was immobilized on the surface of MNP to confirm successful preparation of MNP@TCT (Scheme 1S and Fig. 2S). In the next step, MNP@TCT was subjected to react with 2-aminopyridine. This is the key step and both chlorides must be replaced with 2-aminopyridine to obtain pincer platform MNP@TCT/Amp. Therefore the reaction was performed under reflux condition for complete substitution. The final

catalyst MNP@*NNN*-pincer/Cu was achieved via complexation of CuI with pincer platform in acetonitrile as solvent at room temperature.

To verify the successful incorporation of the organic components and the maintenance of the Si-C bonds during the catalyst preparation, FT-IR spectrum was used in each step. Fig. 1-(I) shows the FT-IR spectra of MNP (a), MNP@APTS (b), MNP@TCT (c), MNP@TCT/Amp (d) and MNP@*NNN*-pincer/Cu (e). Two absorbance bands at 630 and 1090 $cm^{-1}$ in the Fig. 1a-e(I) show stretching frequency of Fe-O and Si-O bonds of MNP that confirmed successful preparation of silica coated $Fe_3O_4$ without changing during all modifications. Region through 1200-1900 $cm^{-1}$ is magnified to clarify the effect of all functionalization steps (Fig. 1-II). Functionalization of MNP with APTS (Fig. 1b-II), was confirmed by the appearance of characteristic bands at 1410 and 1466 $cm^{-1}$ which is related to stretching vibrations of C-N bonds. The FT-IR spectrum of MNP@TCT (Fig. 1c-II) showed strong absorption bands at 1610, 1560, and 1509 $cm^{-1}$ corresponding to C=N of TCT. Stretching absorption of unreacted C-Cl is completely obscured by the bending vibration of the Si-O-Si bond. In the IR spectrum of MNP@TCT/Amp (Fig. 1d-II), comparing to MNP@TCT (Fig.1c-II), the C=N absorption bands shifted to 1656, 1619, and 1542 $cm^{-1}$. This is strong evidence for the presence of several C=N bonds which is the result of the replacement of both of Cl by 2-aminopyridine. Coordination of CuI to the pincer ligand has no effect on the IR spectrum of MNP@*NNN*-pincer/Cu (Fig. 1e-II comparing to its precursor).

Thermogravimetric analysis (TGA) was performed on bare MNP, MNP@APTS, MNP@TCT, and MNP@TCT/Amp (Fig. 2I, a-d) to investigate the organic content of each intermediate and final catalyst. The weight losses through 100-150 ˚C were attributed to the loss of absorbed water

molecules on the surface of all samples. The TGA curve of MNP@APTS (Fig. 2Ib) showed a weight loss at 260 ˚C, which is attributed to the degradation of amino propyl groups. From this weight loss (3.3 wt%), the loading amount of APTS on the surface of MNP was calculated to be 0.56 mmol.$g^{-1}$. Increasing the weight loss in the TGA curve of MNP@TCT to 10.6 wt% (Fig. 2Ic) showed successful incorporation of TCT to amine-functionalized MNP. The Loading amount was also calculated to be 0.48 mmol.$g^{-1}$ for APTS/TCT segment on MNP. The weight loss increased again when MNP@TCT reacted with 2-aminopyridine (13.7 wt%) (Fig. 2I-d). From this weight loss, the loading of *NNN*-pincer ligand on the surface of MNP was calculated to be 0.42 mmol.$g^{-1}$. After complexation of CuI by pincer ligand, no significant change was observed in the TGA carve of MNP@*NNN*-pincer/Cu because of inorganic identity of CuI. From Fig.2I-d, it was found that magnetic pincer ligand is thermally stable up to 270 °C. The DTG analysis of the ligand also showed three peaks at 100, 260 and 340 °C which were attributed to loss of water molecules and organic compartments (Fig. 2II).

The XRD pattern of MNP@*NNN*-pincer/Cu is completely matched with the XRD pattern of the $Fe_3O_4$ standard sample (JCPDS file No. 19-0629), confirming the presence of $Fe_3O_4$ which indicated that all modifications did not change the crystalline phase of $Fe_3O_4$ (Fig. 3a). The broad peak at $2\theta$=20-30 is attributed to the amorphous silica phase in the catalyst structure. The electron ring diffraction pattern (RDP) of the catalyst showed the crystallinity of $Fe_3O_4$ nanoparticles support (Fig. 3b).

Energy-dispersive X-ray analysis (EDX) of MNP@*NNN*-pincer/Cu indicated the presence of C, O, N, Si, Fe, and impotantly Cu elements in the catalyst structure (Fig. 4). From this analysis, it

was found that the amount of Cl is very low in comparison with other element indicated displacment of Cl with aminopyridine in high percentage (third step of catalyst preparation). This analysis also confirms the successful immobilization of the Cu(I) on the surface of MNP by a pincer ligand.

Magnetization property of catalyst was examined using VSM analysis. VSM curves of $Fe_3O_4$, $Fe_3O_4$@$SiO_2$ (MNP) and catalyst MNP@*NNN*-pincer/Cu are shown in Fig. 5a-c, respectively. Reasonable decrease in magnetization intensity of $Fe_3O_4$@$SiO_2$ compared to $Fe_3O_4$ is due to $SiO_2$ layer on $Fe_3O_4$. Magnetic saturation (MS) values 54.5 emu $g^{-1}$ of catalyst showed 15.2 emu $g^{-1}$ diminution compared to MNP which is another claim for functionalization of MNP with organic components. However, the magnetization of catalyst is still enough to respond to an external magnetic field (Fig. 5).

The morphology, particle size, and crystallinity of $Fe_3O_4$ support and MNP@*NNN*-pincer/Cu nanocatalyst were determined by high resolution TEM. Fig. 6a shows the $Fe_3O_4$ dark particles which have an average size of 7 nm. The TEM image of the MNP@*NNN*-pincer/Cu (Fig. 6b) shows gray layer of $SiO_2$ accompanied with organic components around $Fe_3O_4$ particles with an average particle diameter of 17 nm.

The content of Cu(I) in MNP@*NNN*-pincer/Cu was examined by atomic absorption spectroscopy (AAS) using standard samples. It was found that the loading amount of Cu(I) ion in the catalyst structure is 0.38 mmol.$g^{-1}$. The XRF analysis of MNP@ *NNN*-pincer/Cu obtained 2.27 and 4.69 wt% for Cu and I which are corresponded to 0.36 and 0.37 mmol.$g^{-1}$ consisting the result of AAS

for loading of Cu(I). Also, the XRF analysis showed that no significant amount of Cl (0.15 wt%) remained in MNP@ *NNN*-pincer/Cu. These results are in agreement with EDS analysis.

Table 1 shows the elemental analysis of the catalyst MNP@TCT-Amp/Cu. CHN analysis showed that after the reaction of TCT with MNP@APTS, the weight percent of carbon and nitrogen increased, demonstrating the successful attachment of TCT to MNP@APTS. From N content of MNP@APTS (0.76 wt%), the loading of APTS was calculated to be 0.54 $mmol.g^{-1}$ which is along with TGA data. The presence of 3.45 wt% of Cl obtained from the XRF analysis of MNP@TCT proved that only one chloride of TCT was reacted in this step. This also gave the loading 0.50 $mmol.g^{-1}$ for MNP@TCT. The weight percent of N in MNP@TCT/Amp rose again after the reaction of MNP@TCT with 2-aminopyridine (Entry 3). In addition, the weight percent of Cl dramatically decreased, to 0.15 wt% confirming the complete substitution of two Cl with 2-aminopyridine. On complexation of CuI to pincer ligand, no significant change was observed in the %CHN of catalyst compared to its ligand.

*Reactions and scopes*

Elegant recent studies on metal-catalyzed oxidative coupling reactions involving terminal alkynes,[50-60] provided useful starting points for our investigations on the efficiency of MNP@*NNN*-pincer/Cu. Thus, oxidative homocoupling reaction of phenylacetylene was chosen as a model system for optimization studies (Table 2). Initially, the effect of solvent was screened using 1.5 mol% MNP@*NNN*-pincer/Cu in the presence of $Et_3N$ as base (entries 1-5). The reaction exhibited the high activity and 85% yield of product **3a** under solvent free condition. Performing the reaction in MeCN obtained high yield of product while the leaching of Cu(I) was also high. Evaluation of base effect on the reaction under solvent free condition (entries 6-10)

revealed that morpholine is a good base for production of more than 99% yield of product. Since the catalyst has many nitrogen atoms on its surface, we guessed that the catalyst could be also served as a basic catalyst and therefore the reaction could be preceded without any external base. In effect, this claim was true and the reaction obtained relatively good yield of product in the presence of MNP@*NNN*-pincer/Cu without any base, but the catalyst activity decreased in second and third successive runs (entry 9). In the final step, the amount of catalyst loading was explored. It was found that decreasing the catalyst loading to 0.38 mol%, did not effect on the yield of product **3a** (entries 13-17). However, using less than 0.38 mol% loading of catalyst, even with increasing the temperature, the yield of **3a** was diminished (entries 19-21). Thus, condition of entry 17 was chosen as optimized condition. In order to comparison of catalytic activity of the MNP@*NNN*-pincer/Cu to that of the free complex in solution, ligand **A**[61] was prepared and applied in the reaction. The results showed that the use of 0.38 mol% homogeneous catalytic system **A**/CuI gave comparable results with heterogeneous system (entry 18). Apparently, immobilization of pincer catalyst onto the solid support allows easy separation of catalyst from the reaction mixture and importantly several reuse of heterogeneous systems without loss of activity; the factors are not obtained using the homogeneous catalytic systems.

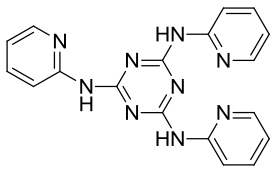

Ligand **A**

Terminal alkyne scope and product diversity were examined using various types of terminal alkynes under optimized conditions (Table 3). As shown in Table 3, aromatic alkynes gave 92-99% yield of 1,3-diynes (**3a-e**) at room temperature using 0.38 mol% of MNP@*NNN*-pincer/Cu.

Aliphatic alkynes also smoothly underwent the reaction to produce 83-92% of **3f-j**, however temperature and catalyst loading must be increased to 60 °C and 0.76 mol%, due to the less reactivity of aliphatic terminal alkynes. In the next experiments, alkyl propiolates were also subjected to the homocoupling reaction under optimized condition. Unfortunately, any attempt failed to produce homocoupling product **3k**. In the presence of morpholine as base, enaminone **4** formed. Examination of tertiary bases resulted in mixture of products (Scheme 3).

Catalytic efficacy of the MNP*@NNN*-pincer/Cu was also examined in the copper catalyzed heterogeneous three-component cycloaddition reaction of alkyl halide, azide, and alkyne, Cu-AAC, known as click reaction.[62-71] The model reaction of benzyl bromide, sodium azide, and phenylacetylene was chosen for optimization of the reaction conditions (Table 4). Different parameters such as solvent, catalyst loading, temperature, and sodium azide amount were tested. As it's evident from Table 4 (entries 1-7), solvent has a major effect on the reaction time and product yield. Under solvent-free condition, reaction did not produce acceptable yield after 12 h. In aprotic solvent, even polar ones, low yield of product was obtained via a long reaction time. Instead, the reaction effectively proceeded in protic solvent, especially $H_2O$. This effect could be attributed to high solubility of $NaN_3$ or ionic intermediates in polar protic solvents. In addition, heterogeneous catalyst MNP*@NNN*-pincer/Cu is highly dispersible in $H_2O$. Water is also a green and cheap solvent. Thus, $H_2O$ was chosen as solvent for further optimization. Optimization of catalyst loading was then examined starting from catalyst-free conditions. Mixture of 1,4- and 1,5-diphenyl-1,2,3-triazoles (3:1, 75%) were obtained after 24 h under reflux condition (entry 8), showing the effect of copper catalyst on selectivity and affectivity of the click reaction. From Table 4, entries 9-15, it was found that catalyst loading, time, and temperature simultaneously

affect on the yield of **5a**. Increasing the time and temperature to 2 h and 50 °C has compensated diminishing of catalyst loading from 0.38 to 0.04 mol% with almost equal yields (Compare entry 6 with 13, Table 4). It was also observed that increasing the amount of $NaN_3$ enhanced the yield of product up to 97%, while increasing the temperature to 80 °C results in a mixture of 1,5- and 1,4-isomers (1:2.7, 81%, entry 15). Consecutively, the most suitable result was obtained for the reaction in the presence of 0.04 mol% MNP@*NNN*-pincer/Cu and 1.3 eq. $NaN_3$ in $H_2O$ at 50 °C (Table 4, entry 14). Application of homogeneous copper catalytic system **A**/CuI was also examined and its activity was compared with MNP@*NNN*-pincer/Cu (entries 16-17). However, the homogeneous catalytic system was as effective as heterogeneous; it suffers from unrecyclability and unreusability.

After finding the optimal reaction conditions, the generality and scope of the click cycloaddition with MNP@*NNN*-pincer/Cu were further explored with diverse alkyl halides and terminal alkynes. With phenylacetylene as substrate (Table 5), 81-98% of product yields were acquired using a variety of benzyl halides (**5a-f**), allyl halide (**5g**), and alkyl halides (**5h-n**). However, benzyl halides with electron donating group exhibited better reaction conditions in time and yield. It is notable that to perform the reaction with non-benzylic halides, $NaN_3$ and temperature were increased to make substitution of azide and halide easier in $H_2O$ (**3k-n**).

Catalyst MNP@*NNN*-Pincer/Cu also showed excellent activity in cycloaddition of aliphatic alkynes (Table 6) with sodium azide and various halides. Because of less reactivity of aliphatic alkynes compared to phenylacetylene, the click reaction with aliphatic proceeded with 0.19

mol% catalyst and 80 °C (Table 6). Again, in the cases of aliphatic halides (Table 6, **6f**-**g**, **k**), the amount of $NaN_3$ must be increased to obtain good yields of product.

Catalytic efficacy of MNP@*NNN*-pincer/Cu was also evaluated using electron-deficient terminal alkynes, which are normally difficult substrates for copper catalyzed click reaction. Good yields of 1-benzyl-1,2,3-triazole-4-alkylcarboxylate **7a**-**b** were obtained with 0.04 mol% Cu-catalyst at 50 °C via 10-12 h (Scheme 4). This product is very interesting from synthetic point of view.[72-76] Click cycloaddition of amino acid-functionalized alkynes **8a**-**b** with benzyl bromide and $NaN_3$ was also tested in the presence of pincer catalyst. As depicted in Scheme 5, good yields of amino acid-functionalized 1,2,3-triazoles **9a**-**b** were obtained under the optimized condition.

To investigate the highest activity of catalyst obtainable for the copper-catalyzed click reaction, another experiment was developed considering Scheme 6. The large scale (10 mmol) reaction of sodium azide, phenylacetylene and benzyl bromide was performed in the presence of 1 mg MNP@PDMA-Cu (0.004 mol%). Surprisingly, excellent yield of 96% was obtained for **5a** after 20 hours (Scheme 5). However, the time for completion of the reaction is relatively high, but calculation of the TON = 25263 and TOF = 1263 $h^{-1}$ shows that the catalyst is truly active and effective. To the best of our knowledge, these values of TOF and TOF for a un-polymeric heterogeneous catalyst have been rarely reported in the click reaction.[77]

Ensuring recyclability of the heterogeneous catalysts while maintaining the catalytic efficiency is a prominent concern in the field of catalysis. Thus, the recyclability of MNP@*NNN*-pincer/Cu

was explored and evaluated in the Cu-AAC reaction of benzyl bromide, $NaN_3$, and phenylacetylene under the optimized condition (Fig. 7a). The recyclability and reusability of the MNP@*NNN*-pincer/Cu were verified in eight consecutive cycles; with slightly decrease in the reactivity observed in the $7^{th}$ and $8^{th}$ cycles. All reactions were carried out in a test tube without separation of catalyst. After each run, the catalyst was carefully collected at the bottom of the test tube by applying an external magnetic field, reaction solution was decanted, and catalyst was washed with MeOH, and utilized directly in the next cycle. Reusability of the catalyst also examined in the aerobic oxidative homocoupling reaction of phenylacetylene (Fig. 1s). The catalyst was recovered and reused up to 6 successive runs without significant loss of activity.

In order to gain insight into the heterogeneous nature of catalyst, the hot leaching test was carried out. The model reaction was performed under optimized conditions and catalyst was quickly collected from the hot solution after 1 h. According to GC analysis of the reaction mixture at different times, as indicated in Fig. 7b, after ignition of the MNP@*NNN*-pincer/Cu no further reaction took place without catalyst. After 3 h from removal of catalyst, the reaction mixture was also analyzed using ICP to determine the content of probable leached Cu(I) in the solution. As expected, because of high power of *NNN*-pincer ligand, no significant amount of Cu(I) was found in the solution demonstrating that MNP@*NNN*-pincer/Cu exhibits a typical heterogeneous catalyst nature. These results are also along with recyclability test.

## Conclusion

In summary, MNP have been easily functionalized with a *NNN*-pincer ligand from TCT/Amp through simple and straightforward convergent protocols. The MNP@TCT-Amp was used as a powerful platform for the construction of nanomagnetic *NNN*-pincer catalyst in combination with Cu(I) that have been immobilized *in situ*. The characterization of the nanocatalyst proved that it was uniformly decorated with mean diameters of 17 nm, exhibiting 0.38 mmol.g$^{-1}$ loading of Cu(I). Investigations on the catalytic activity of MNP@*NNN*-pincer/Cu toward aerobic oxidative homocoupling of terminal alkyne and click reactions showed that catalyst was the best performer to catalyze various types of substrates. In both homocoupling and click processes, routine substrate scope have been carried out with just 0.38 and 0.04 mol% loading, respectively, but click reaction with only 0.004 mol% of catalyst was also possible through larger reaction time, allowing to obtain TON of up to 25,000. This value is higher than those reported with Cu(I) heterogeneous systems, indicating a kind of synergism among the components of the support. Importantly, the nanocatalyst resulted to be recyclable at least 8 times in the click reaction without remarkable loss of activity or significant leaching on Cu(I) according to AAS analysis. Table 7 demonstrates activity and reusability of the present catalyst in comparison with the most recent homogeneous and heterogeneous Cu catalysts in homocoupling reaction. In Table 8, activity and reusability of MNP@NNN-pincer/Cu have been compared with recently reported homogeneous pincer and heterogeneous copper catalysts in the click reaction.

**References**


1. M. Albrecht and G. van Koten, *Angew. Chem. Int. Ed. Engl.*, 2001, **40**, 3750-3781.
2. M. Asay and D. Morales-Morales, *J. Chem. Soc., Dalton Trans.*, 2015, **44**, 17432-17447.
3. H. Li, B. Zheng and K.-W. Huang, *Coord. Chem. Rev.*, 2015, **293**, 116-138.
4. K. J. Szabó, *J. Mol. Catal. A: Chem.*, 2010, **324**, 56-63.
5. C. J. Moulton and B. L. Shaw, *J. Chem. Soc., Dalton Trans.*, 1976, DOI: 10.1039/DT9760001020, 1020-1024.
6. G. van Koten, *Pure Appl. Chem.*, 1989, **61**, 1681-1694.
7. S. Murugesan and K. Kirchner, *J. Chem. Soc., Dalton Trans.*, 2016, **45**, 416-439.
8. H. A. Younus, W. Su, N. Ahmad, S. Chen and F. Verpoort, *Adv. Syn. Catal.*, 2015, **357**, 283-330.
9. D. Yang, Y. Tang, H. Song and B. Wang, *Organometallics*, 2016, **35**, 1392-1398.
10. H. Zhang, Y.-Q. Li, P. Wang, Y. Lu, X.-L. Zhao and Y. Liu, *J. Mol. Catal. A: Chem.*, 2016, **411**, 337-343.
11. X. Lefèvre, G. Durieux, S. Lesturgez and D. Zargarian, *J. Mol. Catal. A: Chem.*, 2011, **335**, 1-7.
12. C. Gunanathan and D. Milstein, *Chem. Rev.*, 2014, **114**, 12024-12087.
13. S. Schneider, J. Meiners and B. Askevold, *Eur. J. Inorg. Chem.*, 2012, **2012**, 412-429.
14. S. Werkmeister, J. Neumann, K. Junge and M. Beller, *Chem. Eur. J.*, 2015, **21**, 12226-12250.
15. G. E. Tyson, K. Tokmic, C. S. Oian, D. Rabinovich, H. U. Valle, T. K. Hollis, J. T. Kelly, K. A. Cuellar, L. E. McNamara and N. I. Hammer, *J. Chem. Soc., Dalton Trans.*, 2015, **44**, 14475-14482.

16. V. Arumugam, W. Kaminsky and D. Nallasamy, *Green Chem.*, 2016, **18**, 3295-3301.

17. D. E. Bellone, J. Bours, E. H. Menke and F. R. Fischer, *J. Am. Chem. Soc.*, 2015, **137**, 850-856.

18. G. A. Filonenko, R. van Putten, E. N. Schulpen, E. J. Hensen and E. A. Pidko, *ChemCatChem*, 2014, **6**, 1526-1530.

19. S. Murugesan, B. Stöger, E. Pittenauer, G. Allmaier, L. F. Veiros and K. Kirchner, *Angew. Chem.*, 2016, **128**, 3097-3100.

20. T. Simler, P. Braunstein and A. A. Danopoulos, *Chem. Commun.*, 2016, **52**, 2717-2720.

21. P. M. P. Garcia, P. Ren, R. Scopelliti and X. Hu, *ACS Catal.*, 2015, **5**, 1164-1171.

22. S. Y. Hong, J. Kwak and S. Chang, *Chem. Commun.*, 2016, **52**, 3159-3162.

23. J. Shi, B. Hu, D. Gong, S. Shang, G. Hou and D. Chen, *J. Chem. Soc., Dalton Trans.*, 2016, **45**, 4828-4834.

24. M. J. Moure, R. SanMartin and E. Domínguez, *Adv. Syn. Catal.*, 2014, **356**, 2070-2080.

25. K. Herasymchuk, J. Huynh, A. J. Lough, L. Roces Fernández and R. A. Gossage, *Synthesis*, 2016, **48**, 2121-2129.

26. B. K. Langlotz, H. Wadepohl and L. H. Gade, *Angew. Chem.*, 2008, **120**, 4748-4752.

27. Q. H. Deng, C. Rettenmeier, H. Wadepohl and L. H. Gade, *Chem. Eur. J.*, 2014, **20**, 93-97.

28. M. B. Gawande, P. S. Branco and R. S. Varma, *Chem. Soc. Rev.*, 2013, **42**, 3371-3393.

29. S. A. Burgess, A. Kassie, S. A. Baranowski, K. J. Fritzsching, K. Schmidt-Rohr, C. M. Brown and C. R. Wade, *J. Am. Chem. Soc.*, 2016, **138**, 1780-1783.

30. A. M. Rasero-Almansa, A. Corma, M. Iglesias and F. Sánchez, *ChemCatChem*, 2013, **5**, 3092-3100.

31. M. Rimoldi, D. Fodor, J. van Bokhoven and A. Mezzetti, *Catal. Sci. Technol.*, 2015, **5**, 4575-4586.

32. C. del Pozo, A. Corma, M. Iglesias and F. Sanchez, *Green Chem.*, 2011, **13**, 2471-2481.

33. B. Tamami, M. M. Nezhad, S. Ghasemi and F. Farjadian, *J. Organomet. Chem.*, 2013, **743**, 10-16.

34. S. Sobhani, Z. Vahidi, Z. Zeraatkar and S. Khodadadi, *RSC. Adv.*, 2015, **5**, 36552-36559.

35. M. Ghotbinejad, A. R. Khosropour, I. Mohammadpoor-Baltork, M. Moghadam, S. Tangestaninejad and V. Mirkhani, *RSC. Adv.*, 2014, **4**, 8590-8596.

36. P. Kang, S. Zhang, T. J. Meyer and M. Brookhart, *Angew. Chem. Int. Ed. Engl.*, 2014, **53**, 8709-8713.

37. M. Ghotbinejad, A. R. Khosropour, I. Mohammadpoor-Baltork, M. Moghadam, S. Tangestaninejad and V. Mirkhani, *J. Mol. Catal. A: Chem.*, 2014, **385**, 78-84.

38. Y. Zhang, X. Sun, H. Zhang and J. Zhao, *Appl. Organomet. Chem.*, 2016, **30**, 645-652.

39. N. Zohreh, S. H. Hosseini, A. Pourjavadi and C. Bennett, *Appl. Organomet. Chem.*, 2016, **30**, 73-80.

40. A. Pourjavadi, S. H. Hosseini, N. Zohreh and C. Bennett, *RSC. Adv.*, 2014, **4**, 46418-46426.

41. N. Zohreh, S. H. Hosseini, A. Pourjavadi and C. Bennett, *RSC. Adv.*, 2014, **4**, 50047-50055.

42. A. Pourjavadi, N. Safaie, S. H. Hosseini and C. Bennett, *New J. Chem.*, 2016, **40**, 1729-1736.

43. H. Veisi, D. Kordestani, S. Hemmati, A. R. Faraji and H. Veisi, *Tetrahedron Lett.*, 2014, **55**, 5311-5314.

44. M. Nasr-Esfahani, I. Mohammadpoor-Baltork, A. R. Khosropour, M. Moghadam, V. Mirkhani, S. Tangestaninejad and H. Amiri Rudbari, *The Journal of organic chemistry*, 2014, **79**, 1437-1443.

45. N. Gupta, T. Roy, D. Ghosh, S. H. R. Abdi, R. I. Kureshy, N.-u. H. Khan and H. C. Bajaj, *RSC. Adv.*, 2015, **5**, 17843-17850.

46. D. Gong, W. Liu, T. Chen, Z.-R. Chen and K.-W. Huang, *J. Mol. Catal. A: Chem.*, 2014, **395**, 100-107.

47. Y. Gartia, A. Biswas, M. Stadler, U. B. Nasini and A. Ghosh, *J. Mol. Catal. A: Chem.*, 2012, **363–364**, 322-327.

48. N. Zohreh, S. H. Hosseini and A. Pourjavadi, *J. Ind. Eng. Chem.*, 2016, **39**, 203-209.

49. A. Pourjavadi, S. H. Hosseini, F. Matloubi Moghaddam, B. Koushki Foroushani and C. Bennett, *Green Chem.*, 2013, **15**, 2913-2919.

50. N. Barot, S. B. Patel and H. Kaur, *J. Mol. Catal. A: Chem.*, 2016, **423**, 77-84.

51. L. Al-Hmoud, S. Bali, S. Mahamulkar, J. Culligan and C. W. Jones, *J. Mol. Catal. A: Chem.*, 2014, **395**, 514-522.

52. B. Maaten, J. Moussa, C. Desmarets, P. Gredin, P. Beaunier, T. Kanger, K. Tõnsuaadu, D. Villemin and M. Gruselle, *J. Mol. Catal. A: Chem.*, 2014, **393**, 112-116.

53. G. Cheng, H. Zhang and X. Cui, *RSC. Adv.*, 2014, **4**, 1849-1852.

54. Y. Liu, N. Gu, P. Liu, J. Xie, X. Ma, Y. Liu and B. Dai, *Appl. Organomet. Chem.*, 2015, **29**, 736-738.

55. F.-W. Li, Q.-L. Suo, H.-L. Hong, N. Zhu, Y.-Q. Wang, L.-L. Guo and L.-M. Han, *J. Supercrit. Fluids*, 2014, **92**, 70-74.

56. S. Biswas, K. Mullick, S.-Y. Chen, D. A. Kriz, M. Shakil, C.-H. Kuo, A. M. Angeles-Boza, A. R. Rossi and S. L. Suib, *ACS Catal.*, 2016, **6**, 5069-5080.

57. S. Yan, S. Pan, T. Osako and Y. Uozumi, *Synlett*, 2016, **27**, 1232-1236.

58. X.-L. Shi, Q. Hu, F. Wang, W. Zhang and P. Duan, *J. Catal.*, 2016, **337**, 233-239.

59. M. Nasr-Esfahani, I. Mohammadpoor-Baltork, A. R. Khosropour, M. Moghadam, V. Mirkhani, S. Tangestaninejad, V. Agabekov and H. A. Rudbari, *RSC. Adv.*, 2014, **4**, 14291-14296.

60. S. Li, X. Chen, J. Chen and H. Gong, *Bull. Chem. Soc. Jpn.*, 2016, **89**, 794-797.

61. S. Mandal, G. Bérubé, É. Asselin, I. Mohammad, V. J. Richardson, A. Gupta, S. K. Pramanik, A. L. Williams and S. K. Mandal, *Bioorg. Med. Chem. Lett.*, 2007, **17**, 4955-4960.

62. B. Gröll, P. Schaaf, M. D. Mihovilovic and M. Schnürch, *J. Mol. Catal. A: Chem.*, DOI: http://dx.doi.org/10.1016/j.molcata.2016.07.013.

63. A. Akbari, N. Arsalani, M. Amini and E. Jabbari, *J. Mol. Catal. A: Chem.*, 2016, **414**, 47-54.

64. D. P. Singh, B. K. Allam, K. N. Singh and V. P. Singh, *J. Mol. Catal. A: Chem.*, 2015, **398**, 158-163.

65. I. Jlalia, F. Gallier, N. Brodie-Linder, J. Uziel, J. Augé and N. Lubin-Germain, *J. Mol. Catal. A: Chem.*, 2014, **393**, 56-61.

66. S. Gu, D. Xu and W. Chen, *J. Chem. Soc., Dalton Trans.*, 2011, **40**, 1576-1583.

67. S. Y. de Boer, Y. Gloaguen, M. Lutz and J. I. van der Vlugt, *Inorg. Chim. Acta*, 2012, **380**, 336-342.

68. T. Cheisson and A. Auffrant, *J. Chem. Soc., Dalton Trans.*, 2014, **43**, 13399-13409.

69. C. Wang, D. Wang, S. Yu, T. Cornilleau, J. Ruiz, L. Salmon and D. Astruc, *ACS Catal.*, 2016, **6**, 5424-5431.

70. X. Liu, N. Novoa, C. Manzur, D. Carrillo and J.-R. Hamon, *New J. Chem.*, 2016, **40**, 3308-3313.

71. A. Pourjavadi, S. H. Hosseini, F. Matloubi Moghaddam and S. E. Ayati, *RSC. Adv.*, 2015, **5**, 29609-29617.

72. H. Duan, D. Arora, Y. Li, H. Setiadi, D. Xu, H.-Y. Lim and W. Wang, *Bioorg. Med. Chem.*, 2016, **24**, 2621-2630.

73. J. Zeidler, D. Baraniak and T. Ostrowski, *Eur. J. Med. Chem.*, 2015, **97**, 409-418.

74. H. Cheng, J. Wan, M.-I. Lin, Y. Liu, X. Lu, J. Liu, Y. Xu, J. Chen, Z. Tu and Y.-S. E. Cheng, *J. Med. Chem.*, 2012, **55**, 2144-2153.

75. C. W. Tornøe, S. J. Sanderson, J. C. Mottram, G. H. Coombs and M. Meldal, *J. Comb. Chem.*, 2004, **6**, 312-324.

76. F. d. C. da Silva, M. C. B. V. de Souza, I. I. P. Frugulhetti, H. C. Castro, S. L. d. O. Souza, T. M. L. de Souza, D. Q. Rodrigues, A. M. T. Souza, P. A. Abreu, F. Passamani, C. R. Rodrigues and V. F. Ferreira, *Eur. J. Med. Chem.*, 2009, **44**, 373-383.

77. Y. M. A. Yamada, S. M. Sarkar and Y. Uozumi, *J. Am. Chem. Soc.*, 2012, **134**, 9285-9290.

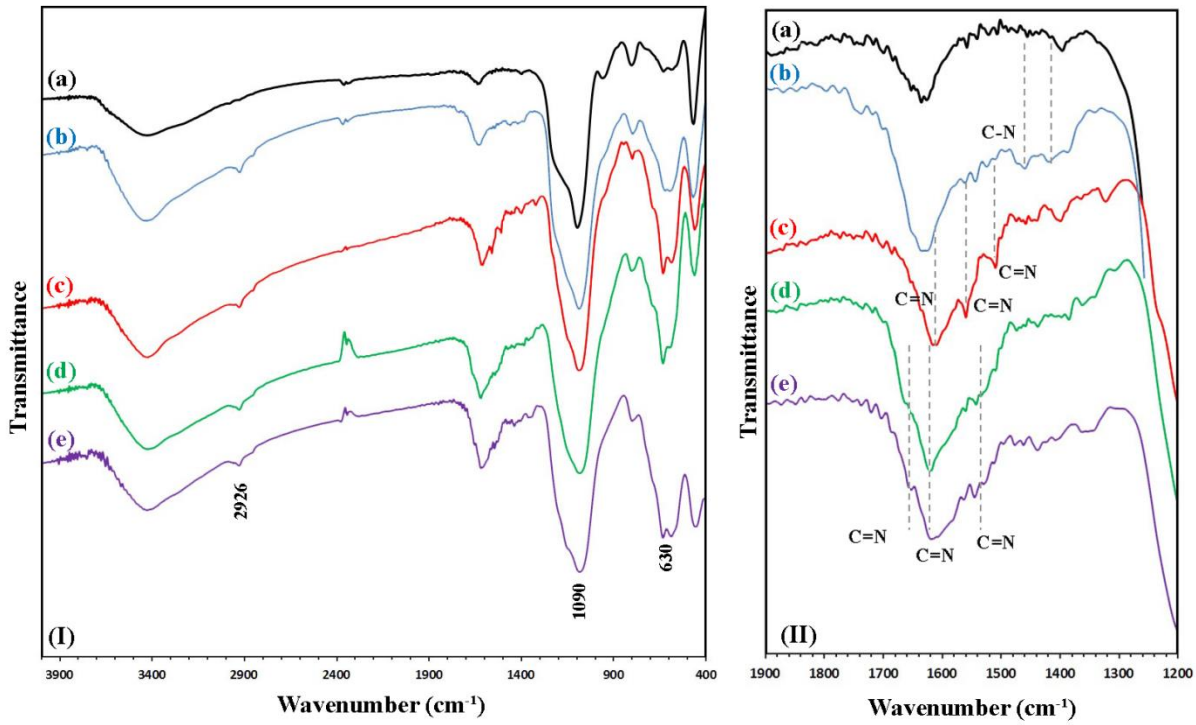


**Fig. 1.** FT-IR spectra of MNP (a), MNP@APTS (b), MNP@TCT (c), MNP@TCT/Amp (d) and MNP@*NNN*-pincer/Cu (e); (I): normal range 400-4000 $cm^{-1}$, (II): magnified region 1200-1900 $cm^{-1}$.

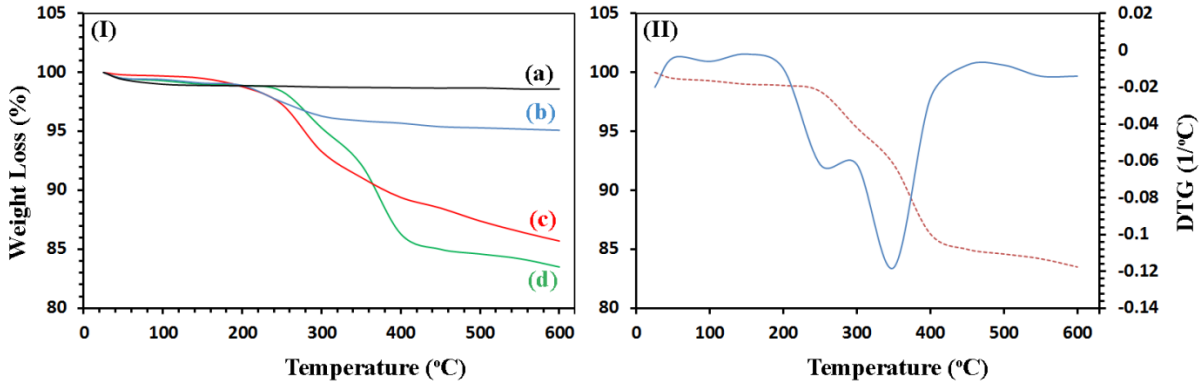


**Fig. 2.** (I) TGA curves of bare MNP (a), MNP@APTS (b), MNP@TCT (c), MNP@TCT/Amp (d); (II) DTG curve of MNP@TCT/Amp.

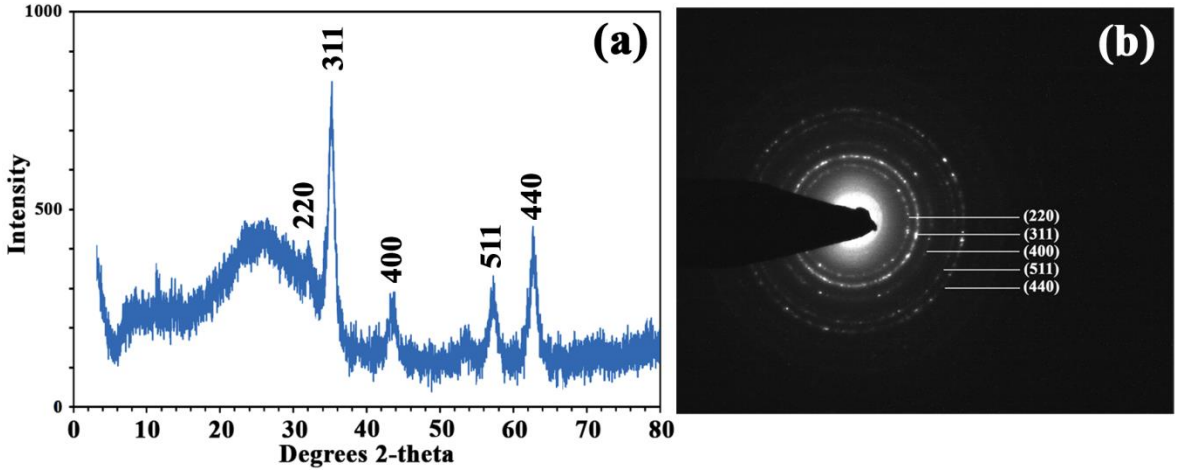


**Fig. 3.** XRD (a) and RDP (b) patterns of the MNP@*NNN*-pincer/Cu.

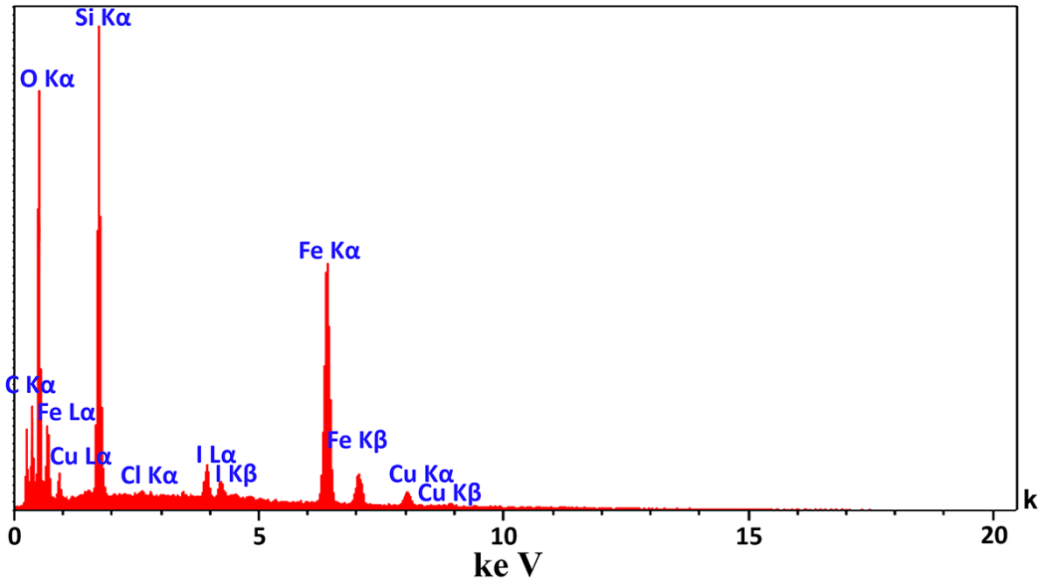


**Fig. 4.** The EDX analysis of MNP@*NNN*-pincer/Cu

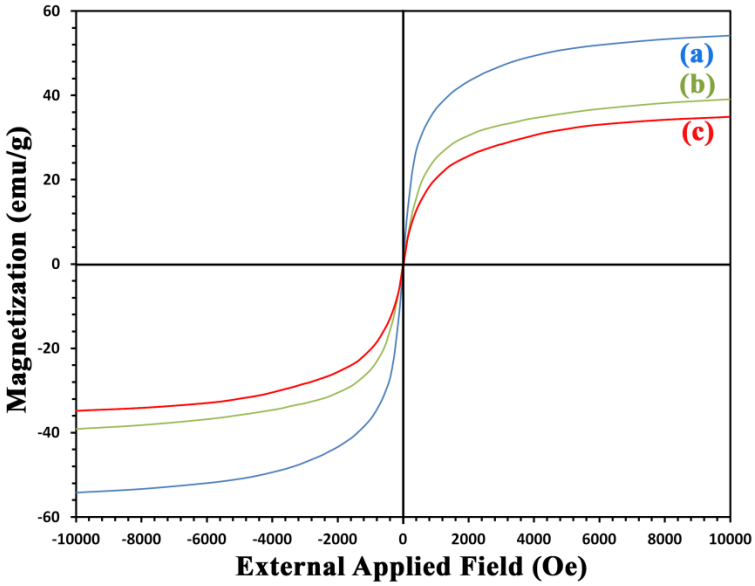


**Fig. 5.** VSM curves for $Fe_3O_4$ (a), MNP (b) and MNP@*NNN*-pincer/Cu (c).

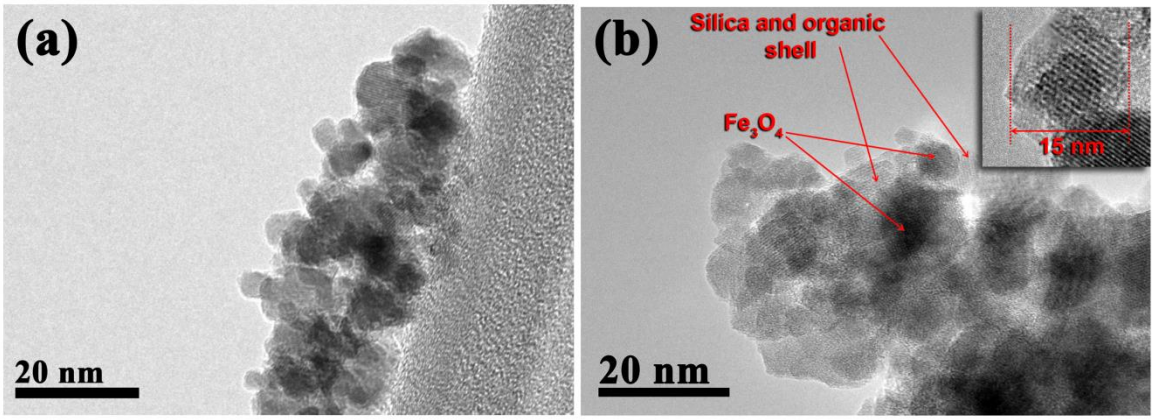


**Fig. 6.** TEM image of $Fe_3O_4$ (a) and catalyst MNP@*NNN*-pincer/Cu (b)

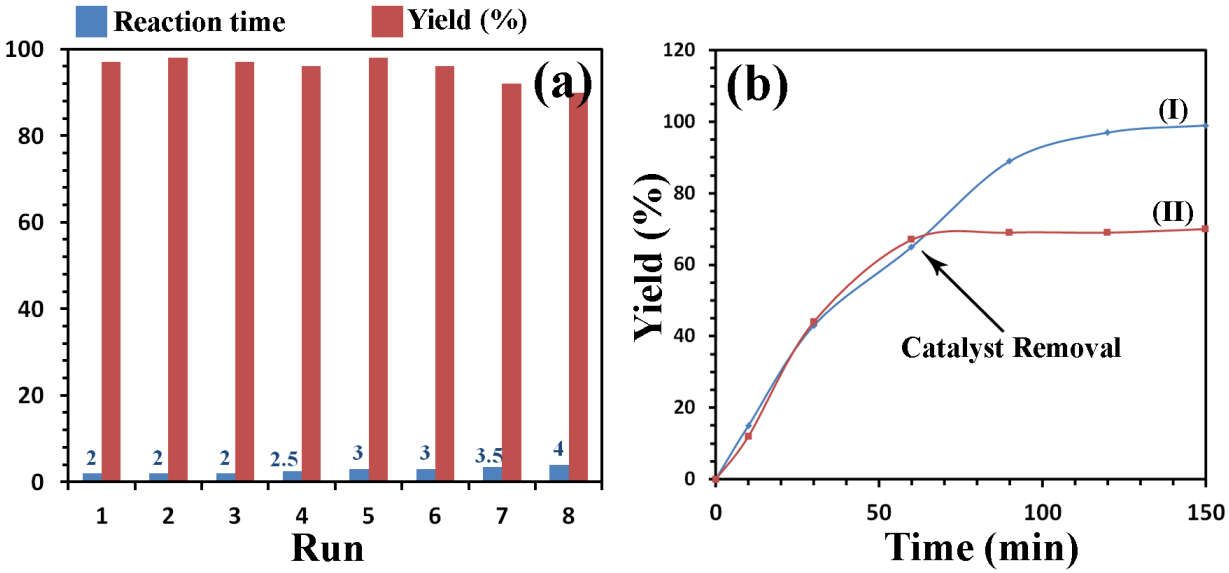


**Fig. 7.** Results of recyclability and leaching experiment of MNP@*NNN*-pincer/Cu in the click reaction

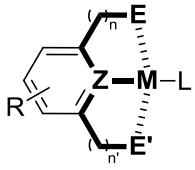


Z: C, N, ... (nutral or anionic)
n and n'= 1, 2
n=n' or n≠n'
E and E': P, N, S, O, and carbens
R= H or preferrely ERG

**Scheme 1.** General structure for pincer metal complexes

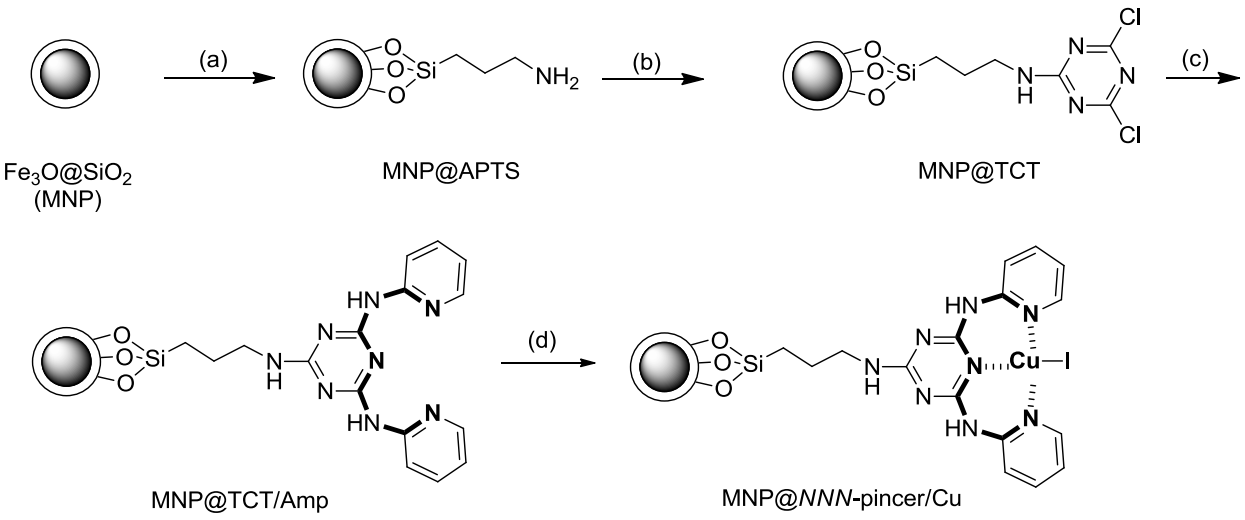


(a): APTS, EtOH, 80 $^{o}$C, 24 h
(b): $C_3N_3Cl_3$, DIEA, super dry THF, 0 $^{o}$C, 2 h
(c): aminopyridine, dry MeCN, reflux, 12 h
(d): CuI, MeCN, r.t., 12 h

**Scheme 2.** Synthetic procedure of MNP@*NNN*-pincer/Cu

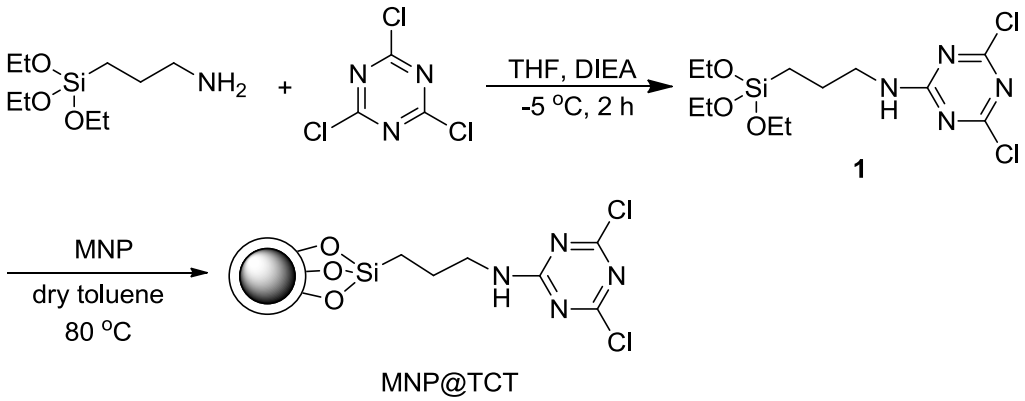


**Scheme 3.** Preparation of MNP@TCT via immobilization of **1** on MNP

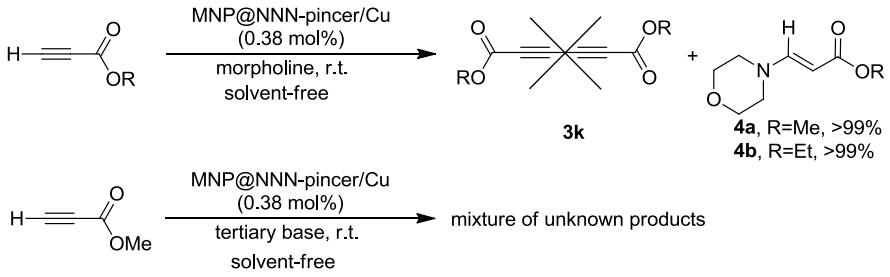


**Scheme 3.** The scope of alkyl acetylenecarboxylates (propiolates) in the oxidative homocoupling reaction using MNP@*NNN*-pimcer/Cu

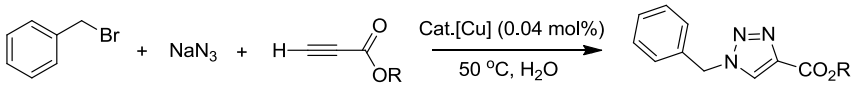


**7a**: R=Me, 77%, 12 h
**7b**: R=Et, 80%, 10 h

**Scheme 4.** Synthesis of 1-benzyl-1,2,3-triazole-4-alkylcarboxylates with MNP@*NNN*-pincer/Cu

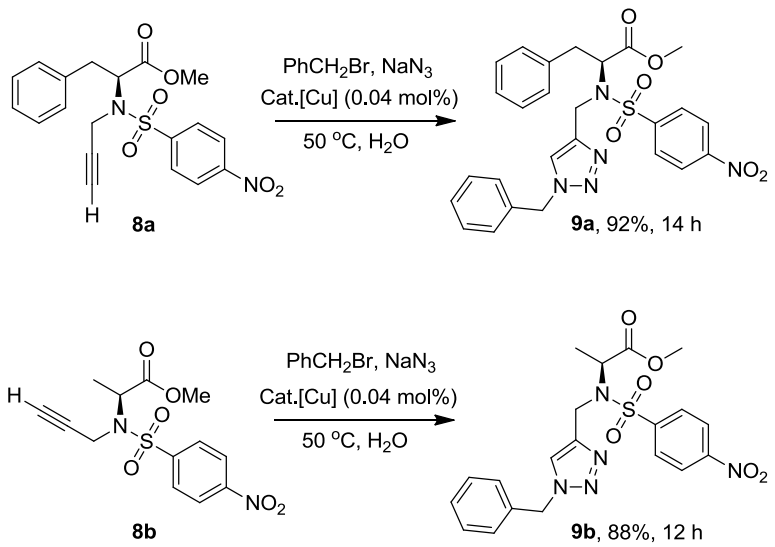


**Scheme 5.** Synthesis of amino acid functionalized-1,2,3-triazoles with MNP@*NNN*-pincer/Cu

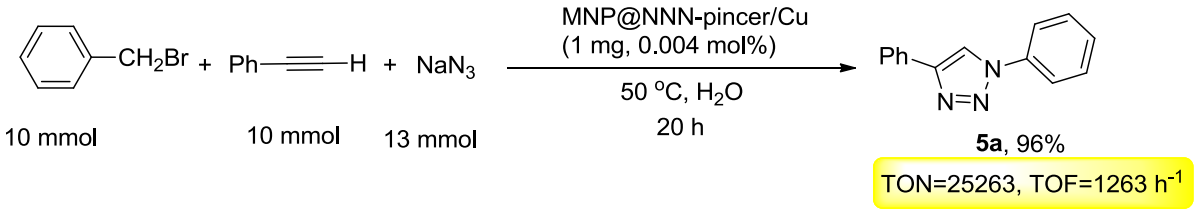


**Scheme 6.** Investigation on the highest activity of catalyst obtainable with 0.004 mol% catalyst

Table 1. The results for elemental analysis of catalyst

| Entry | Sample | %C[a] | %H[a] | %N[a] | %Other element[b] | Loading (mmol/g) |
|---|---|---|---|---|---|---|
| 1. | MNP@APTS | 2.62 | 1.47 | 0.76 | - | 0.54 |
| 2. | MNP@TCT | 4.10 | 1.69 | 2.81 | Cl: 3.45 | 0.50 |
| 3. | MNP@TCT-Amp | 8.83 | 2.52 | 4.58 | Cl: 0.15 | 0.41 |
| 4. | MNP@*NNN*-pincer/Cu | 8.22 | 1.93 | 4.45 | Cu: 2.27<br>I: 4.69 | 0.36 |

[a]Calculated by CHN analyzer.
[b]Obtained from XRF analysis.

**Table 2.** Optimization of various reagents and conditions for aerobic oxidative homocoupling of phenylacetylene using MNP@*NNN*-pincer/Cu[a].

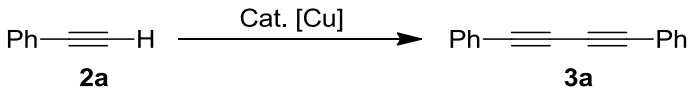


**2a** **3a**

| Optimization | Entry | Cat. (mol%) | Solvent | Base | *T* (°C) | Time (h) | Yield **3a** %[b] |
|---|---|---|---|---|---|---|---|
| Solvent | 1 | 1.5 | $H_2O$ | $Et_3N$ | r.t. | 11 | 63 |
| | 2 | 1.5 | $CH_2Cl_2$ | $Et_3N$ | r.t | 8 | 57 |
| | 3 | 1.5 | MeCN | $Et_3N$ | r.t | 3 | 81[c] |
| | 4 | 1.5 | - | $Et_3N$ | r.t | 3 | 85 |
| | 5 | 1.5 | Toluene | $Et_3N$ | r.t | 15 | 42 |
| Base | 6 | 1.5 | - | DIPEA | r.t | 7 | 77 |
| | 7 | 1.5 | - | $K_2CO_3$ | r.t | 17 | trace |
| | 8 | 1.5 | - | morpholine | r.t. | 1 | > 99 |
| | 9 | 1.5 | - | - | r.t. | 7, 18, 24 | 85, 39, 0[d] |
| | 10 | 1.5 | | DABCO | r.t. | 4 | 80 |
| Catalyst loading | 11 | - | - | morpholine | 80 | 24 | - |
| | 12 | MNP@TCT-Amp (40 mg) | - | morpholine | 80 | 24 | - |
| | 13 | 1 | - | morpholine | r.t. | 1 | > 99 |
| | 14 | 0.9 | - | morpholine | r.t. | 1 | > 99 |
| | 15 | 0.8 | - | morpholine | r.t. | 2 | >99 |
| | 16 | 0.6 | - | morpholine | r.t. | 2.5 | > 99 |
| | **17** | **0.38** | - | **morpholine** | **r.t.** | **2.5** | **> 99 (81[e])** |
| | 18 | 0.38 (**A**:CuI, 1:1) | MeCN | morpholine | r.t. | 3 | >99[f] |
| | 19 | 0.2 | - | morpholine | r.t | 7 | 92 |
| Temperature | 20 | 0.2 | - | morpholine | 50 | 5 | 94 |
| | 21 | 0.2 | - | morpholine | 80 | 5 | 95 |

[a]Reaction condition: phenylacetylene (1 mmol), base (1.2 mmol), solvent (2 mL for entries 1-3, 5).
[b]GC yield.
[c]Leaching is high.
[d]Yields are for three successive runs starting with 40 mg catalyst.
[e]Isolated yield.
[f]Reaction condition: phenylacetylene (1 mmol), morpholine (1.2 mmol), MeCN (2 mL), ligand **A** (0.38 mol%), CuI (0.38 mol%).

**Table 3**. Synthesis of 1,3-diynes using MNP@*NNN*-pincer/Cu[a,b]

| Condition A | | Condition B | |
|---|---|---|---|
| 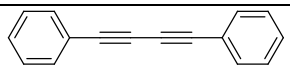 | **3a**, 99 (94)%, 2.5 h | 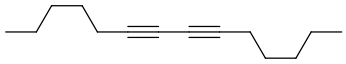 | **3f**, 90 (75)%, 12 h |
| 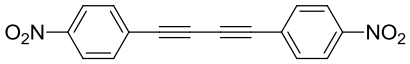 | **3b**, 95%, 2.5 h | 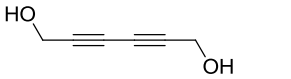 | **3g**, 92%, 15 h |
| 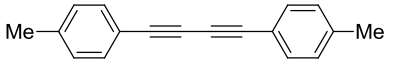 | **3c**, 99%, 3 h | 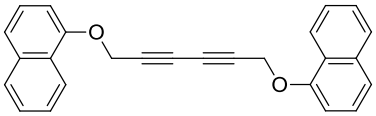 | **3h**, 83%, 9 h |
| 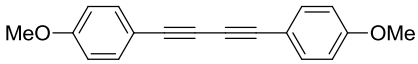 | **3d**, 92%, 3.5 h | 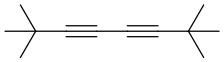 | **3i**, 85%, 10 h |
| 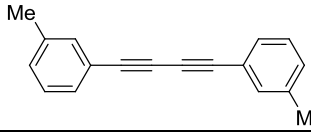 | **3e**, 94%, 3 h | 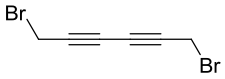 | **3j**, 72%, 10 h |

[a]GC Yields; isolated yields are in parentheses.

[b]Reaction conditions, A: terminal alkyne (1 mmol), morpholine (1.2 mmol), MNP@*NNN*-pincer/Cu (0.38 mol%), r.t, solvent-free; B: terminal alkyne (1 mmol), morpholine (1.2 mmol), MNP@*NNN*-pincer/Cu (0.76 mol%), 60 °C, solvent free.

**Table 4.** Optimization of reaction conditions for the click reaction using MNP@*NNN*-pincer/Cu[a]

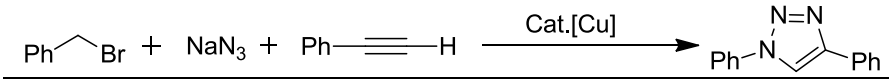


| Entry | Solvent | Cat. (mol%) | *T* (°C ) | Time ( h ) | $NaN_3$ ( eq ) | Yield ( % )[b] |
|---|---|---|---|---|---|---|
| 1 | - | 0.38 | r.t | 12 | 1 | 20 |
| 2 | DMF | 0.38 | r.t | 8 | 1 | 41 |
| 3 | $CH_3CN$ | 0.38 | r.t | 12 | 1 | 15 |
| 4 | $CH_2Cl_2$ | 0.38 | r.t | 9 | 1 | trace |
| 5 | MeOH | 0.38 | r.t | 7 | 1 | 45 |
| 6 | $H_2O$ | 0.38 | r.t | 1.5 | 1 | 81 (92) |
| 7 | MeOH:$H_2O$ (1:1) | 0.38 | r.t | 5 | 1 | 55 |
| 8 | $H_2O$ | - | reflux | 24 | 1 | 75[c] |
| 9 | $H_2O$ | 0.2 | r.t | 2.5 | 1 | 78 (88) |
| 10 | $H_2O$ | 0.12 | r.t | 2.5 | 1 | 85 |
| 11 | $H_2O$ | 0.12 | r.t | 4 | 1 | 76 (90) |
| 12 | $H_2O$ | 0.04 | r.t | 5 | 1 | 81 (91) |
| 13 | $H_2O$ | 0.04 | 50 | 2 | 1 | 82 (95) |
| **14** | **$H_2O$** | **0.04** | **50** | **2** | **1.3** | **90 (97)** |
| 15 | $H_2O$ | 0.04 | 70 | 1.5 | 1.3 | 81 |
| 16 | $H_2O$ | 0.04 (**A**/CuI, 1:1) | 50 | 1.5 | 1.3 | 88[d] |
| 17 | $H_2O$ | 0.04 (**A**/CuI, 1:1) | r.t. | 2 | 1.3 | 82[d] |

[a]Reaction conditions: benzyl bromide (1 mmol), phenylacetylene (1 mmol), solvent (2 mL)
[b]Yields are based on isolated products; yields in parentheses are based on GC analysis.
[c]Mixture of regioisomers.
[d]Reaction conditions: benzyl bromide (1 mmol), phenyl acetylene (1 mmol), $H_2O$ (2 mL), ligand **A** (0.04 mol%), CuI (0.04 mol%).

**Table 5.** Synthesis of 4-phenyl-1,2,3-triazle derivatives using MNP@*NNN*-pincer/Cu[a,b]

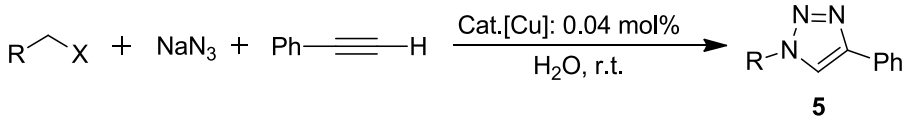


**5**

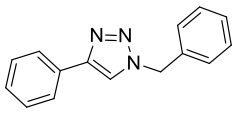

**5a**: X=Br, 97 (90)%, 2 h
X=Cl, 95%, 2 h
X=OTs, 95%, 1.5 h

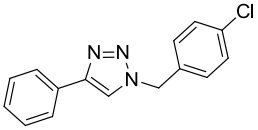

**5b**: X=Cl, 92%, 3.5 h

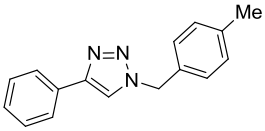

**5c**: X=Cl, 98 (92)%, 2.5 h

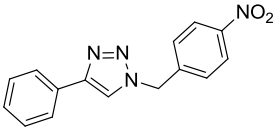

**5d**: X=Cl, 91%, 3 h

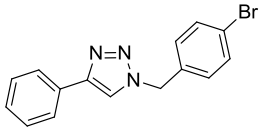

**5e**: X=Br, 95 (82)%, 2 h

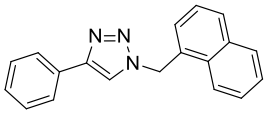

**5f**: X=Cl, 95 (79)%, 1.5 h

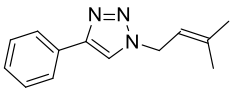

[c]**5g**: X=Br, 90 (83)%, 8 h
X=Cl, 88%, 10 h

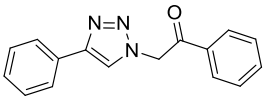

**5h**: X=Br, 91 (80)%, 6 h

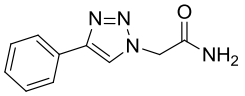

**5i**: X= Br, 91 (77)%, 5 h

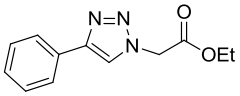

**5j**: X=Br, 90 (85)%, 6 h

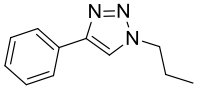

[c]**5k**: X=Cl, 85 (70)%, 12 h

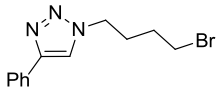

[c]**5l**: X=Br, 88 (70)%, 12 h

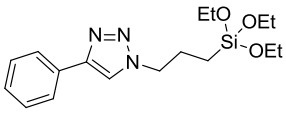

[c]**5m**: X=Cl, 81 (75)%, 15 h

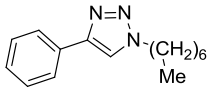

[c]**5n**: X=Br, 85%, 12 h

[a]Reaction Condition: phenylacetylene (1 mmol), $NaN_3$ (1.3 mmol), halide (1 mmol), catalyst (1 mg, 0.04 mol%), $H_2O$ (2 mL), 50 °C. [b]Yields are based on GC analysis; values in parentheses are isolated yields.[c]$NaN_3$ (3 mmol), 80 °C.

**Table 6.** Synthesis of 4-alkyl-1,2,3-triazole derivatives using MNP@*NNN*-pincer/Cu[a,b]

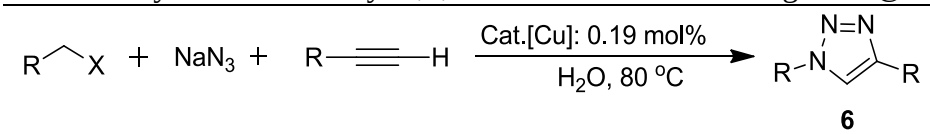


**6**

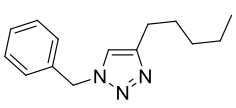

**6a**: X=Br, 87 (80)%, 8 h
X=Cl, 81 (72)%, 10 h

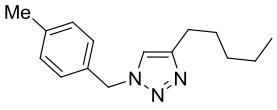


**6b**: X=Cl, 82 (71)%, 7 h

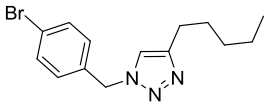


**6c**: X=Br, 85 (77)%, 7 h

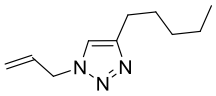

**6d**: X=Br, 89 (70)%, 9 h

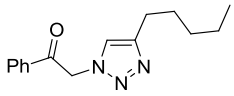


**6e**: X=Br, 81%, 7.5 h

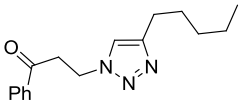


[c]**6f**: X=Br, 83%, 10 h

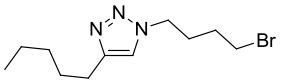


[c]**6g**: X=Br, 88%, 12 h

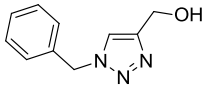


**6h**: X=Br, 84%, 8 h

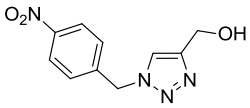


**6i**: X=Br, 80%, 13 h

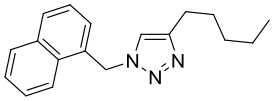

**6j**: X=Br, 80 (73)%, 10 h

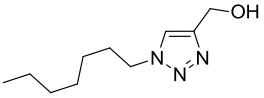


[c]**6k**: X=Br, 82%, 10 h

[a]Reaction Condition: terminal alkyne (1 mmol), $NaN_3$ (1.3 mmol), halide (1 mmol), catalyst (5 mg, 0.19 mol%), $H_2O$ (2 mL), 80 °C. [b]Yields are based on GC analysis; values in parentheses are isolated yields.[c]$NaN_3$ (3 mmol).

**Table 7.** Comparing catalytic activity of MNP@NNN-pincer/Cu with homogeneous and heterogeneous copper catalysts in the aerobic oxidative homocoupling of terminal alkynes

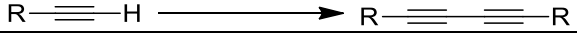

| | | | |
|---|---|---|---|
| Homogeneous catalysts | | | |
| $Cu(CF_3CO_2)_2.H_2O$ (20 mol%), [BMIm][Br] (0.6 eq.), $H_2O$, 50 °C, 24 h, unrecoverable[60] | CuI (2 mol%), $PdCl_2$ (0.1 mol%), $P(Ph)_2CH_2CH_2CO_2H$ (0.2 mol%), r.t., $Et_3N$, DMF, 24 h, unrecoverable[54] | CuCl (5 mol%), DBU (250 mol%), $ScCO_2$ (8 MPa), $O_2$ (1 MPa), unrecoverable[55] | CuI (0.5 mol%), benzylamine (5 mol%), solvent-free, r.t., $O_2$, unrecoverable[53] |
| Heterogeneous catalysts | | | |
| Meso Cu/MnOx (6 mol%), air, toluene, 105 °C, recoverable (filtration), reusable ( 8 runs)[56] | PS-TEDETA-$CuSO_4$ (10 mol%), piperidine (1 eq.), toluene, air, 60 °C, 24 h, recoverable (filtration), reusable (9 runs)[57] | PANFTA.CuI (2 mol%), n-$BuNH_2$ (0.5 eq.), AcOEt, air, r.t. 12 h, recoverable (tweezers), reusable (16 runs)[58] | Cu(II)-TD@nSiO2 (0.6 mol%), DBU (20 mol%), MeCN, r.t., air, 1-3 h, recoverable (filtration), reusable (8 runs)[59] |
| This work: | | | |
| MNP@NNN-pincer/Cu (0.38-0.76 mol%), morpholine (1 eq.), r.t.-60 °C, solvent free, 2.5-15 h, recoverable (external magnet), reusable (6 runs). | | | |

**Table 8.** Comparing catalytic activity of MNP@NNN-pincer/Cu with homogeneous and heterogeneous copper catalysts in the click reaction

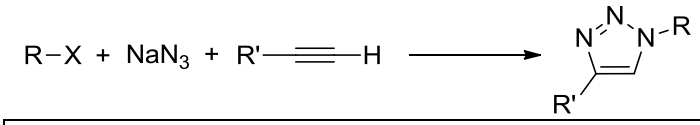


| | | | |
|---|---|---|---|
| Homogeneous catalysts | | | |
| PNP-pincer/Cu complex (1 mol%), 60 °C, super dry $Et_2O$, 16 h, unrecoverable[67] | NNN-pincer/Cu complex (0.1 mol%), $CH_2Cl_2$, r.t., $N_2$, 0.5 h, unrecoverable [68] | NNC-pincer/Cu complex (2 mol%), DMF, $N_2$, 80 °C, 5 h, unrecoverable [66] | $[Cu_2(bpoh)(PPh_3)_4]\cdot$(0.1 mol%), MeCN, r.t., 3 h, unrecoverable[64] |
| Heterogeneous catalysts | | | |
| PEG-tristrz-CuI (20 ppm), $H_2O$, $N_2$, 35 °C, 20 h, recoverable (filtration), reusable (6 runs)[69] | PMMA-supported Schiff base/Cu(II) (2 mol%), Na-ascorbate (20 mol%), EtOH, $N_2$, r.t., 24 h, recoverable (filtration), reusable (4 runs)[70] | POSS-SAL-Cu (II) (2.6 mol%), $H_2O$, 70 °C, recoverable (filtration), reusable (4 runs)[63] | P[imCu/IL][Cl] (0.1 mol%), $H_2O/^tBuOH$, 55 °C, 2 h, recoverable (filtration), reusable (12 runs)[71] |
| This work: | | | |
| MNP@NNN-pincer/Cu (0.38-0.76 mol%), r.t.-60 °C, solvent free, 2.5-15 h, recoverable (external magnet), reusable (8 runs) | | | |